

X-716-65-392

N66-17250

FACILITY FORM 65

(ACCESSION NUMBER) 44
(PAGES)
(NASA CR OR TMX OR AD NUMBER)

(THRU) 1
(CODE) 03
(CATEGORY)

NASA TM X-55377

CHARACTERISTICS OF THE SOLAR ARRAYS FOR THE ENERGETIC PARTICLE EXPLORERS

BY
LUTHER W. SLIFER, JR.
RALPH M. SULLIVAN
NICOLAS V. MEJIA, JR.

GPO PRICE \$ _____

CFSTI PRICE(S) \$ _____

Hard copy (HC) 2.00

Microfiche (MF) .50

OCTOBER 1965

ff 653 July 65



————— GODDARD SPACE FLIGHT CENTER —————
GREENBELT, MARYLAND

CHARACTERISTICS OF THE SOLAR ARRAYS FOR
THE ENERGETIC PARTICLE EXPLORERS

by

Luther W. Slifer, Jr.
Ralph M. Sullivan
Nicolas V. Mejia, Jr.

October 1965

Goddard Space Flight Center
Greenbelt, Maryland

CHARACTERISTICS OF THE SOLAR ARRAYS FOR THE ENERGETIC PARTICLE EXPLORERS

by

Luther W. Slifer, Jr.
Ralph M. Sullivan
Nicolas V. Mejia, Jr.

ABSTRACT

The electrical and mechanical characteristics of the solar arrays, solar paddles, solar cells and some other solar paddle components have been compiled for the Explorer XII, XIV, XV, and XXVI satellites. The characteristics are presented so as to point up the similarities and differences in the solar arrays and afford a correlation of the design features and the requirements leading to those features. These comparisons also illustrate the development in the state of the art of solar arrays and solar cells for the period from 1960 to 1963. One table, which can be used for feasibility studies, etc., of general characteristics such as packing factor, power density, specific power, etc., is presented for the individual solar paddles and another is presented for the solar arrays.

The predicted air mass zero power based on air mass one measurements is presented and compared to telemetered data from the spacecraft. The comparison was within 5% although it was anticipated to be only within 10%. It is shown that the final utilization efficiency of the solar cells was less than 1% and several areas where future efforts should be concentrated are suggested in order to improve this figure.

CONTENTS

	<u>Page</u>
ABSTRACT.....	iii
INTRODUCTION	1
SPACECRAFT CONFIGURATION	1
SPACECRAFT ORBIT AND LIFETIME.....	6
SOLAR ARRAY CONFIGURATION	6
SOLAR PADDLE CONFIGURATION	8
PADDLE POWER OUTPUT.....	16
SOLAR ARRAY POWER OUTPUT	16
GENERAL CHARACTERISTICS	21
SUMMARY AND CONCLUSIONS.....	24
RECOMMENDATIONS.....	26
ACKNOWLEDGMENTS	27
REFERENCES.....	27
APPENDIX A - Spacecraft Nomenclature	28
APPENDIX B - Methods of Correcting and Extrapolating Earth Surface Sunlight Measurements on Solar Paddles to Space Conditions	29
APPENDIX C - Solar Array Calibration	33

LIST OF TABLES

<u>Table</u>		<u>Page</u>
I	Nominal Electrical Load Characteristics for the Energetic Particle Explorers from Initial Orbit Data	1
II	Launch, Orbit, and Lifetime Data for the Energetic Particle Explorers	6
III	Solar Paddle Weights	13
IV	Mechanical Characteristics of the Solar Paddles	14
V	Electrical Configuration of the Solar Paddles	15
VI	Calculated Normal-Incidence, Space Power Output for the Solar Paddles	17
VII	Comparison of Predicted Power and Initial Space Power	21
VIII	General Undegraded Solar Paddle Characteristics at Air Mass Zero	22
IX	General Solar Array Characteristics-Design Performance	23
A1	Names and Designations of the Energetic Particle Explorers	28
C1	Comparison of Methods for Space Power Output Calibration.	34

LIST OF ILLUSTRATIONS

<u>Figure</u>		<u>Page</u>
1	The Explorer XII Spacecraft (on pedestal)	2
2	The Explorer XIV Spacecraft	3
3	The Explorer XV Spacecraft (on pedestal)	4
4	The Explorer XXVI Spacecraft (on spin-rig mount)	5
5	Simplified Block Diagram of Energetic Particle Explorer Electrical System	5
6	Sketch of the "High-Low" Solar Array Configuration for Explorers XII, XIV, and XXVI	7
7	Sketch of the "Flat" Solar Array Configuration for Explorer XV	9
8	An Explorer XII Solar Paddle (in handling frame)	10
9	An Explorer XIV Solar Paddle (in handling frame)	11
10	An Explorer XV or Explorer XXVI Solar Paddle	12
11	Theoretical Effective Paddle Area	18
12	Space Power Output for Explorers XII, XIV, and XXVI	19
13	Space Power Output for Explorer XV	20

CHARACTERISTICS OF THE SOLAR ARRAYS FOR THE ENERGETIC PARTICLE EXPLORERS

INTRODUCTION

Four Energetic Particle Explorer satellites (Explorers XII, XIV, XV and XXVI) were launched between 1961 and 1965. These spacecraft were similar in many respects including many similarities in both the spacecraft loads and the power supplies for those loads. However, in order to improve power output, to improve reliability, and stability of the solar array, to accommodate differences in the satellite orbits, and to compensate for effects of the Starfish high-altitude nuclear explosion, significant differences in the design of the solar arrays were required.

Because of the particular combination of similarities in the spacecraft, differences in the solar arrays and reasons for the differences, the characteristics of the solar arrays are interesting in combination as well as individually.

SPACECRAFT CONFIGURATION

The spacecraft configurations of Explorers XII, XIV, XV and XXVI are shown in Figures 1, 2, 3, and 4, respectively. (Alternate designations for these spacecraft are given in Appendix A.) In these figures the similarity of the mechanical configuration of the spacecraft is readily evident, the only major difference being the solar paddle configuration on Explorer XV, which will be discussed later. The basic electrical system for the spacecraft is shown (in highly simplified form) in Figure 5. This system was typical for all of the above spacecraft. Table I shows the nominal electrical characteristics for each of the spacecraft.

Table I
Nominal Electrical Load Characteristics for the Energetic
Particle Explorers from Initial Orbit Data

Spacecraft	Nominal Current* (milliamps)	Nominal Voltage (volts)	Nominal Power* (watts)
Explorer XII	660	19.6	12.9
Explorer XIV	590	19.9	11.7
Explorer XV	570	19.6	11.2
Explorer XXVI	690	19.4	13.4

*Excluding variable battery charging requirements.

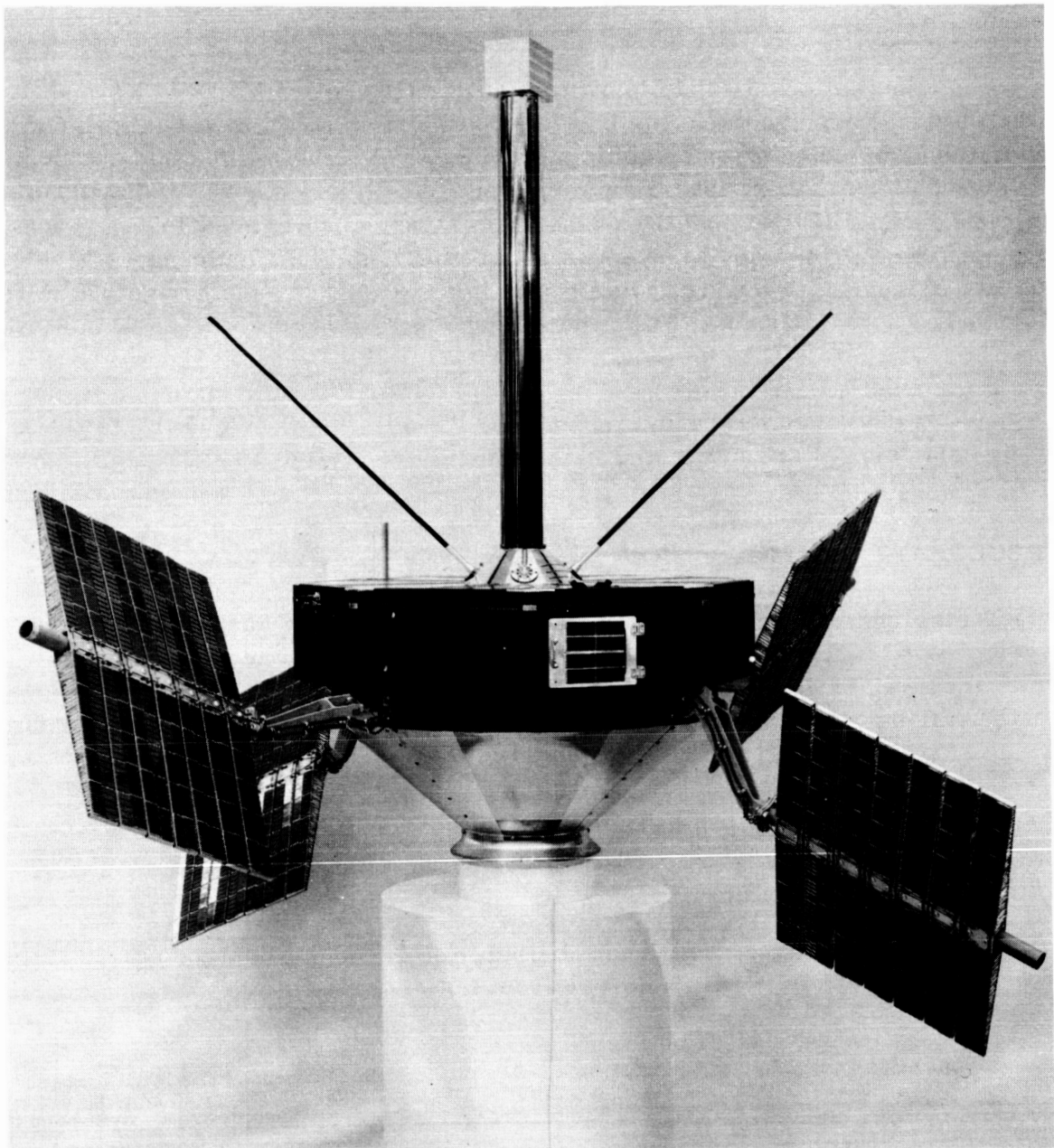


Figure 1—The Explorer XII Spacecraft (on pedestal)

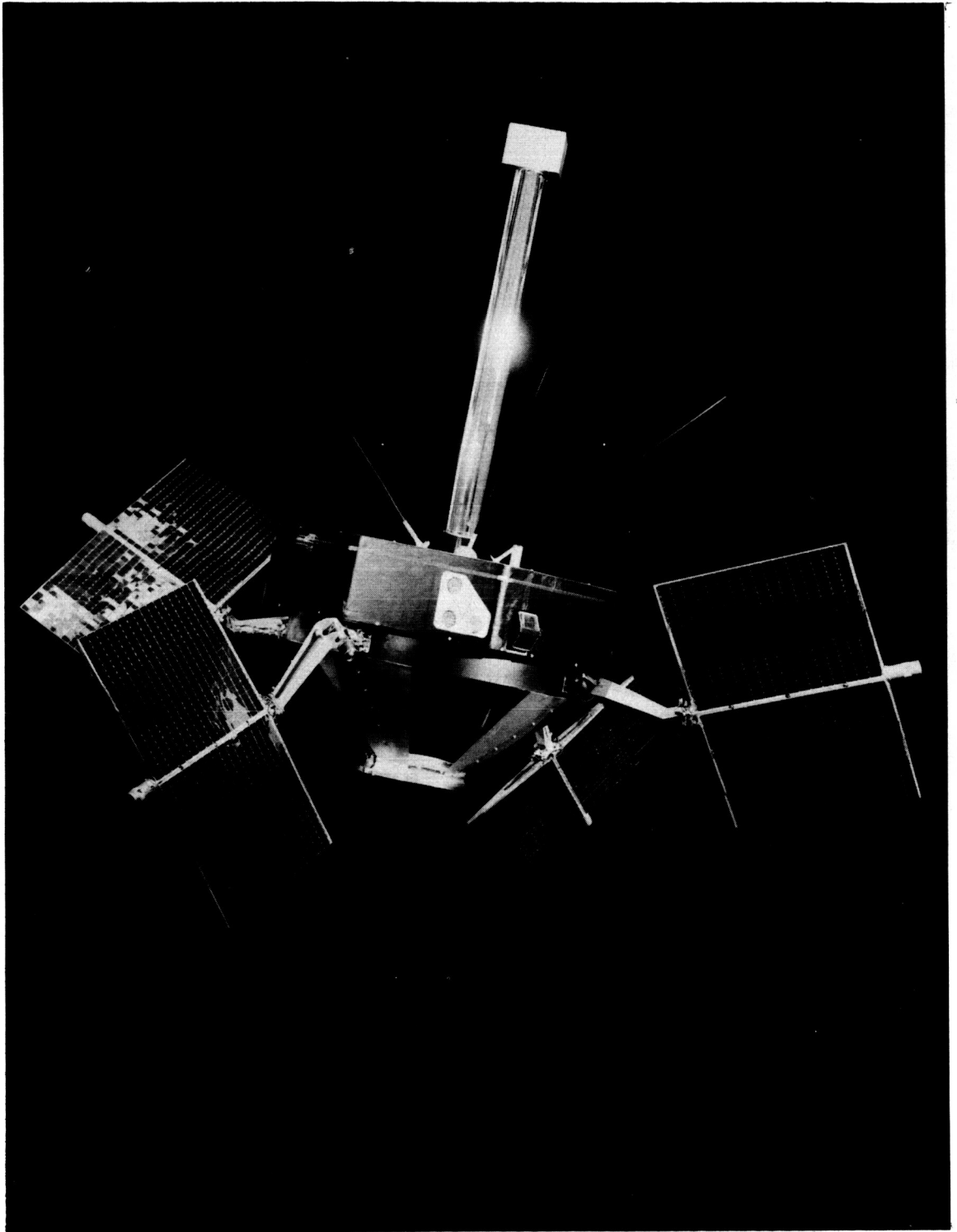


Figure 2—The Explorer XIV Spacecraft

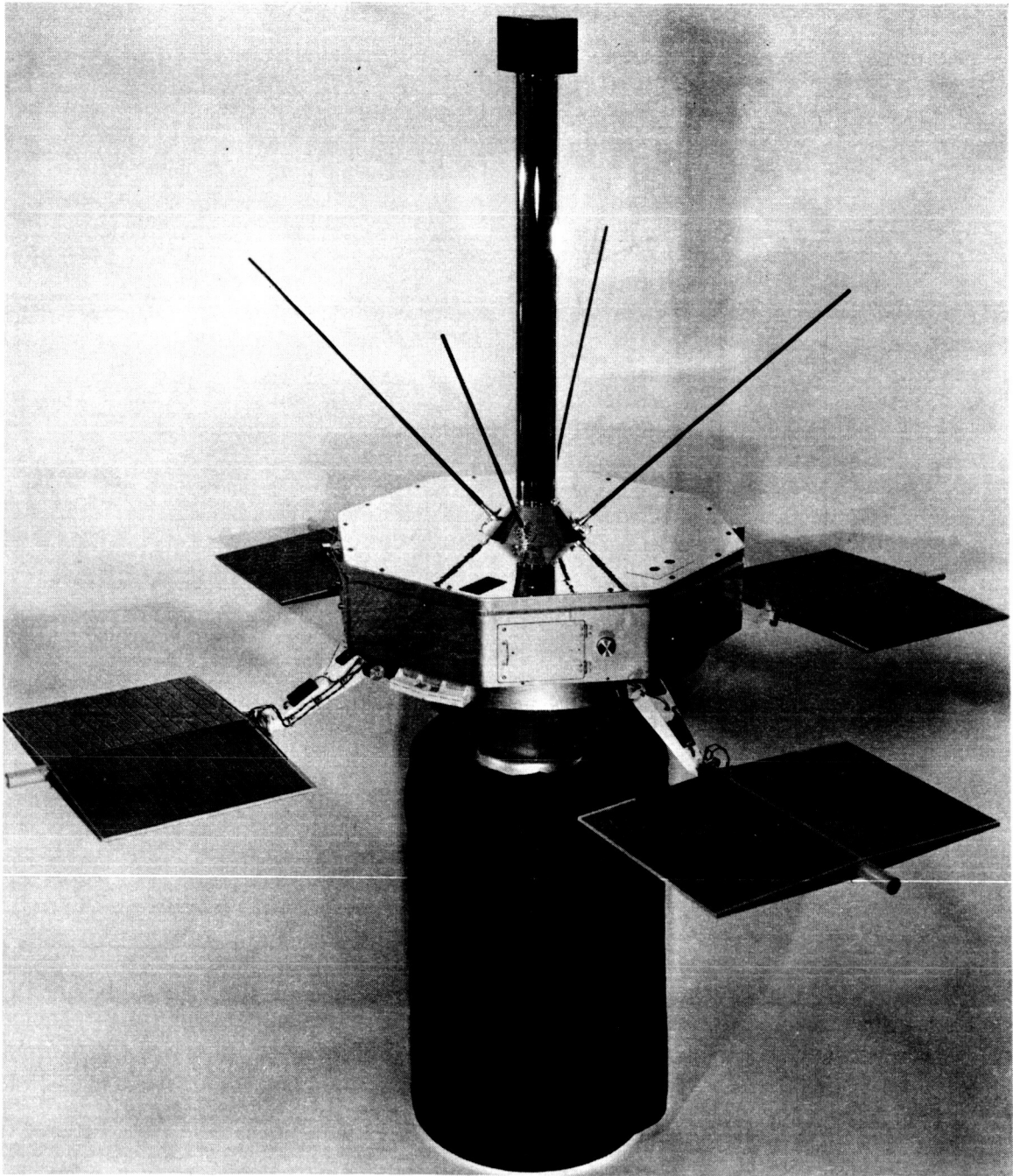


Figure 3—The Explorer XV Spacecraft (on pedestal)

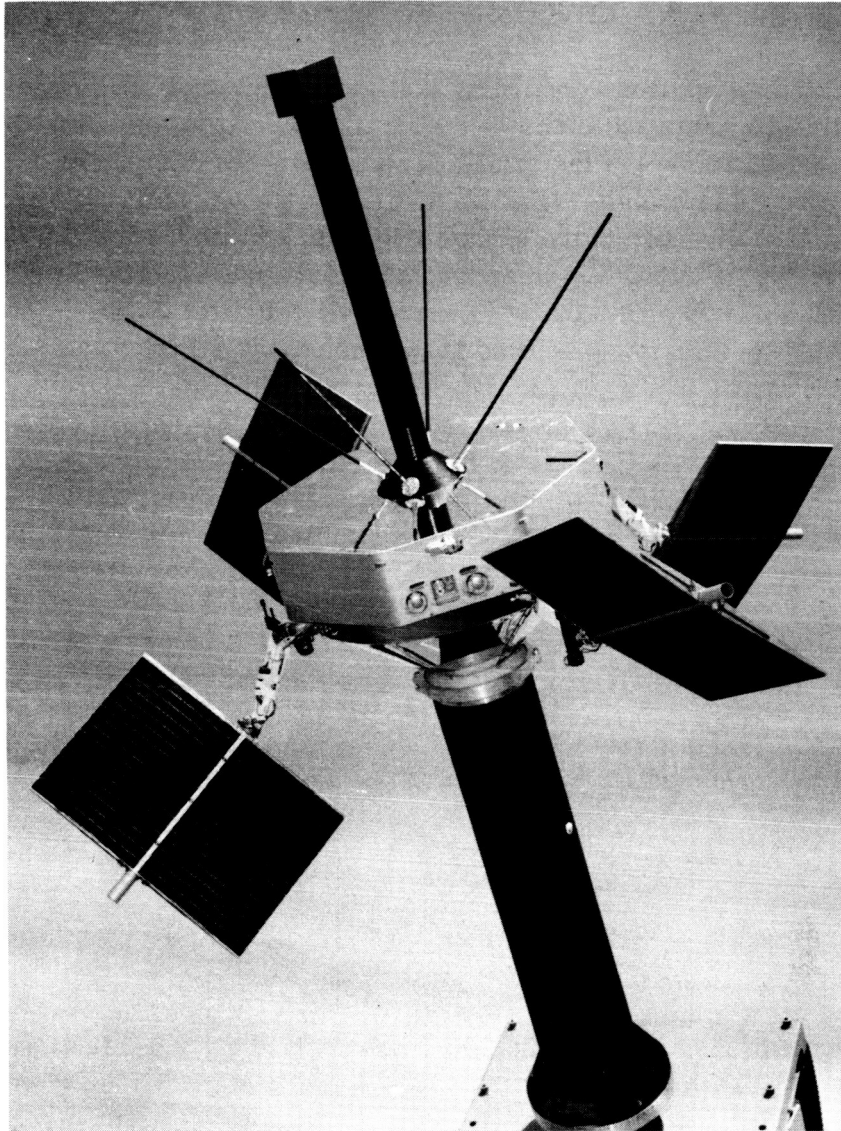


Figure 4—The Explorer XXVI Spacecraft (on spin-rig mount)

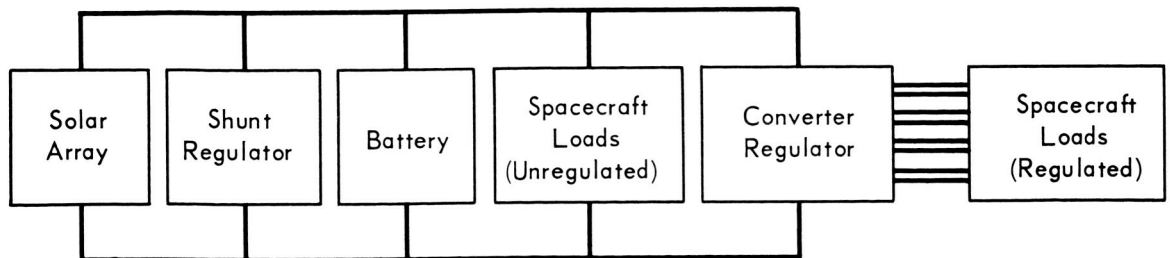


Figure 5—Simplified Block Diagram of Energetic Particle Explorer Electrical System

SPACECRAFT ORBIT AND LIFETIME

Fundamental information concerning the launch and orbit of these spacecraft is shown in Table II. This table shows the similarity of the low-radiation orbits for Explorers XII and XIV and the similarity of orbits for Explorers XV and XXVI, which were subjected to a high-radiation level. It also shows the distinct differences in orbits for these two pairs of satellites. In addition, it shows that the solar array for Explorer XII was designed and flown prior to Starfish; the array for Explorer XIV was designed prior to but flown soon after Starfish; the array for Explorer XV was both designed and flown soon after Starfish; and the array for Explorer XXVI was designed soon after Starfish but flown much later.

Table II
Launch, Orbit and Lifetime Data for the
Energetic Particle Explorers

Spacecraft Name (Explorer)	Launch Date	Initial Orbit Parameter				Lifetime	
		Perigee (km)	Apogee (km)	Incl. (deg)	Period (hours)	Design (days)	Actual (days)
XII*	8/16/61	294	77,340	33	26.5	180-365	112
XIV*	10/2/62	278	98,850	33	36.6	365-730	500
XV**	10/27/62	313	17,640	18	5.3	60	104
XXVI**	12/21/64	309	26,200	20	7.6	365-730	> 270 (Still Operating)

*Solar paddles designed prior to Starfish (July 9, 1962)

**Solar paddles designed immediately after Starfish.

SOLAR ARRAY CONFIGURATION

Each of the Energetic Particle Explorer satellites was powered by means of four identical solar paddles. Two different configurations were used for the solar arrays.

The first configuration, used for Explorers XII, XIV and XXVI, is sketched in Figure 6. It was patterned after the Pioneer V assembly. The paddles were positioned at 90° angles around the body of the spacecraft and extended outward.

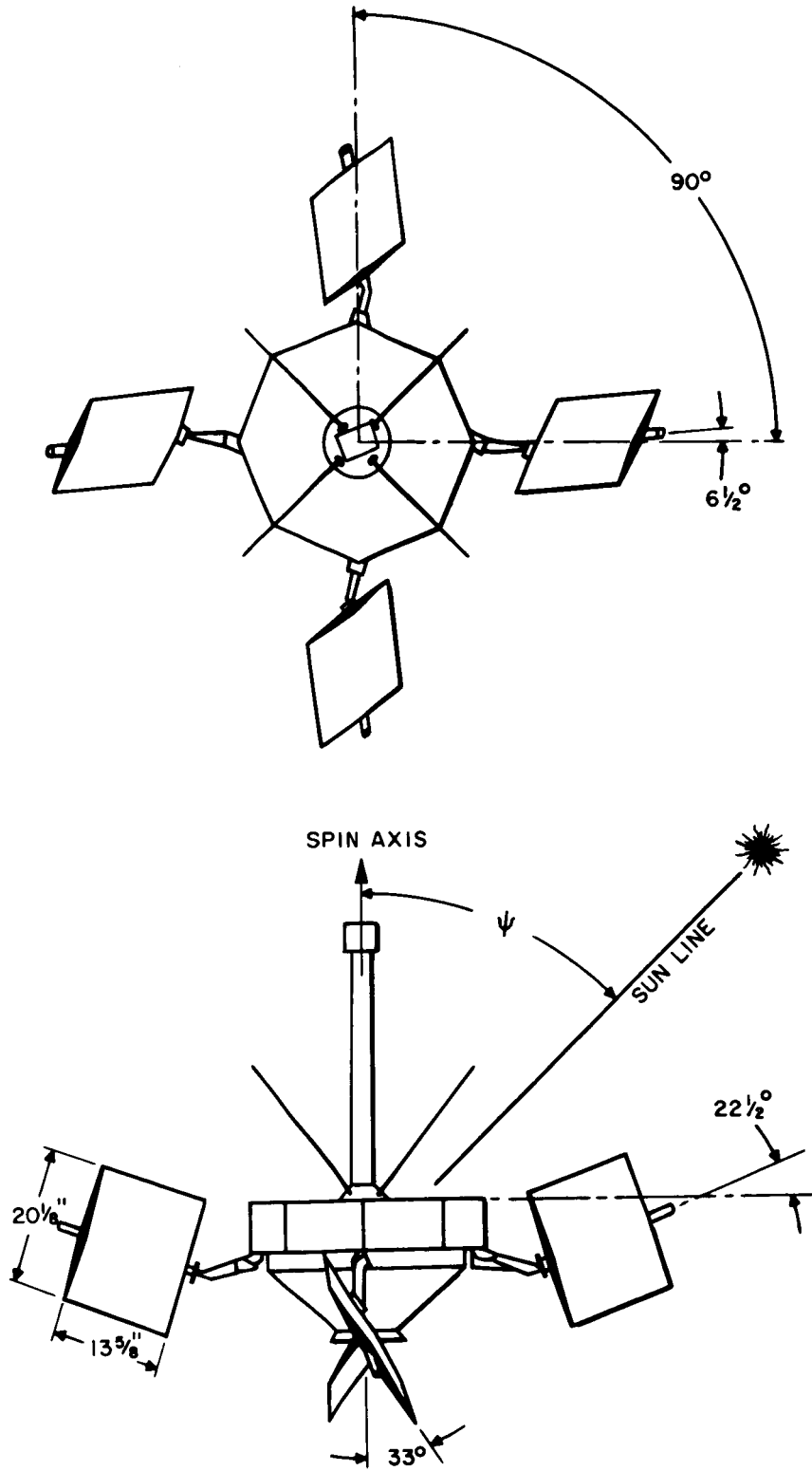


Figure 6—Sketch of the “High-Low” Solar Array Configuration for Explorers XII, XIV, and XXVI

Two of these, diametrically opposite to each other, were erected to an angle of $+22-1/2^\circ$ with respect to a plane parallel to the satellite's equator, and the other two were erected to an angle of $-22-1/2^\circ$ with this plane, giving rise to the terminology of the "high-low" configuration. All four paddles were pitched at an angle of 33° to the vertical plane passing through the spar (centerline) of the paddle. Finally, each spar was canted $6-1/2^\circ$ to a radial line from the center of the spacecraft.

The second configuration, used for Explorer XV, was a "flat" configuration as shown in Figure 7. The paddles extended radially outward from the spin-axis of the satellite at 90° angles around the spacecraft. Each paddle was erected to a 90° angle and pitched to a 90° angle with the result that all four paddles were in a plane parallel to the satellite equator.

The primary reason for the difference in configuration was that the "high-low" paddle configuration was designed for long life and arbitrary sun angle, while the "flat" paddle configuration was designed for short life with maximum power and for sunline controlled (by launch window choice) to angles not significantly off from the spin axis. In addition, it was possible to revert from the "flat" array of Explorer XV to the "high-low" array for Explorer XXVI, in spite of the fact that longer life was required in a similar orbit and the paddles themselves were unchanged, because of the decay of the artificial radiation belt during the time between launchings.

SOLAR PADDLE CONFIGURATION

The configuration of the solar paddles for the four satellites is best described by reference to Figures 8, 9, and 10. In addition, significant mechanical characteristics are given in Tables III and IV, and characteristics pertinent to the electrical configuration are given in Table V.

The Explorer XII paddles (Figure 8) were patterned after the Pioneer V design. The primary difference was the addition of two modules on each paddle because of increased power requirements. These paddles consisted of a main spar at one end of which was a flange for mounting the paddle to the spacecraft. Seven wedge-shaped, aluminum honeycomb modules with aluminum skins were mounted to each side of the spar. Solar cells were mounted on both faces of the module in a 50-cell string composed of ten 5-cell shingles. Protective cover glasses, 6 mil thick, were mounted on the cells for radiation protection. Each string was isolated from all others with a 1N645 blocking diode also mounted on the surface of the module.

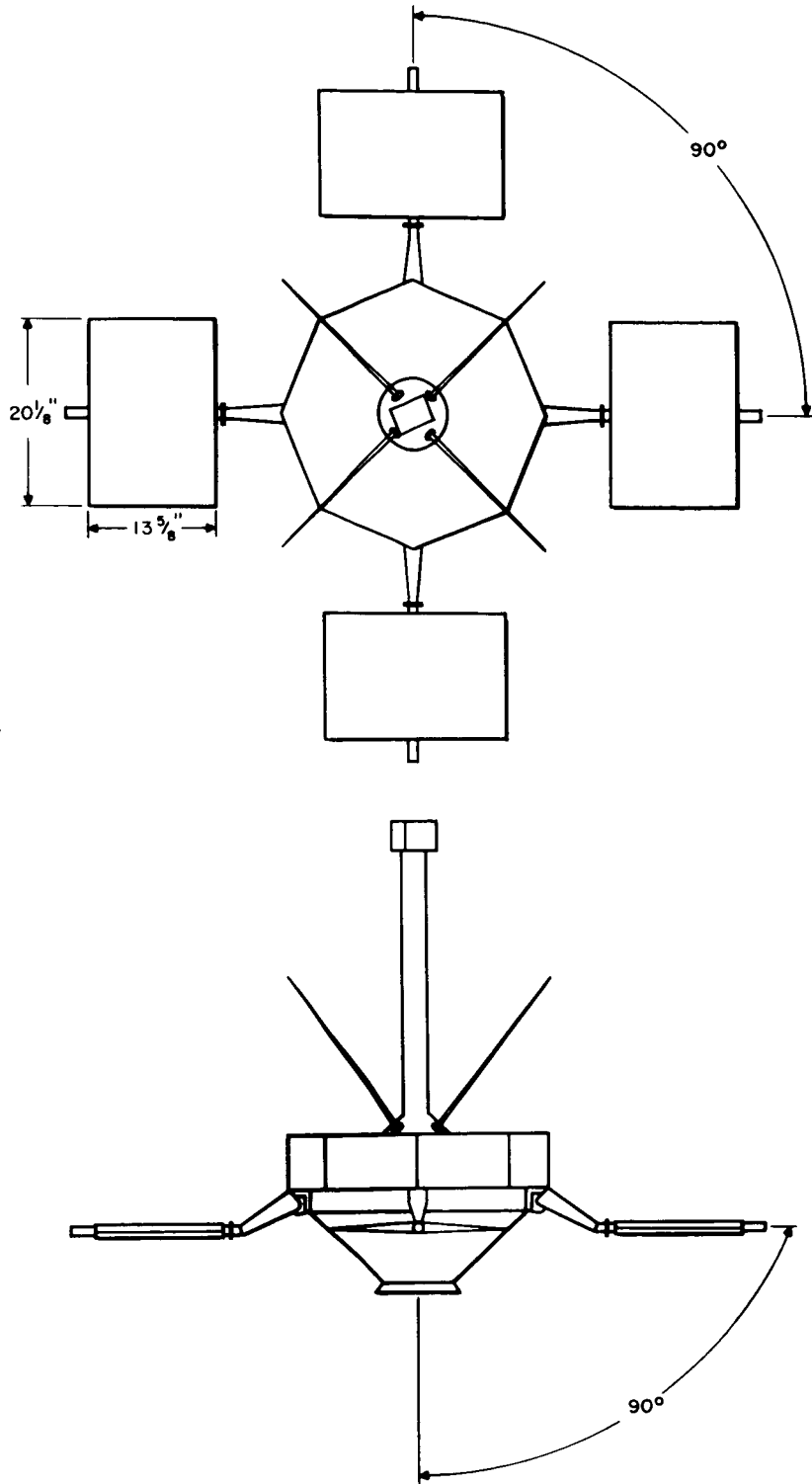


Figure 7-Sketch of the "Flat" Solar Array Configuration for Explorer XV

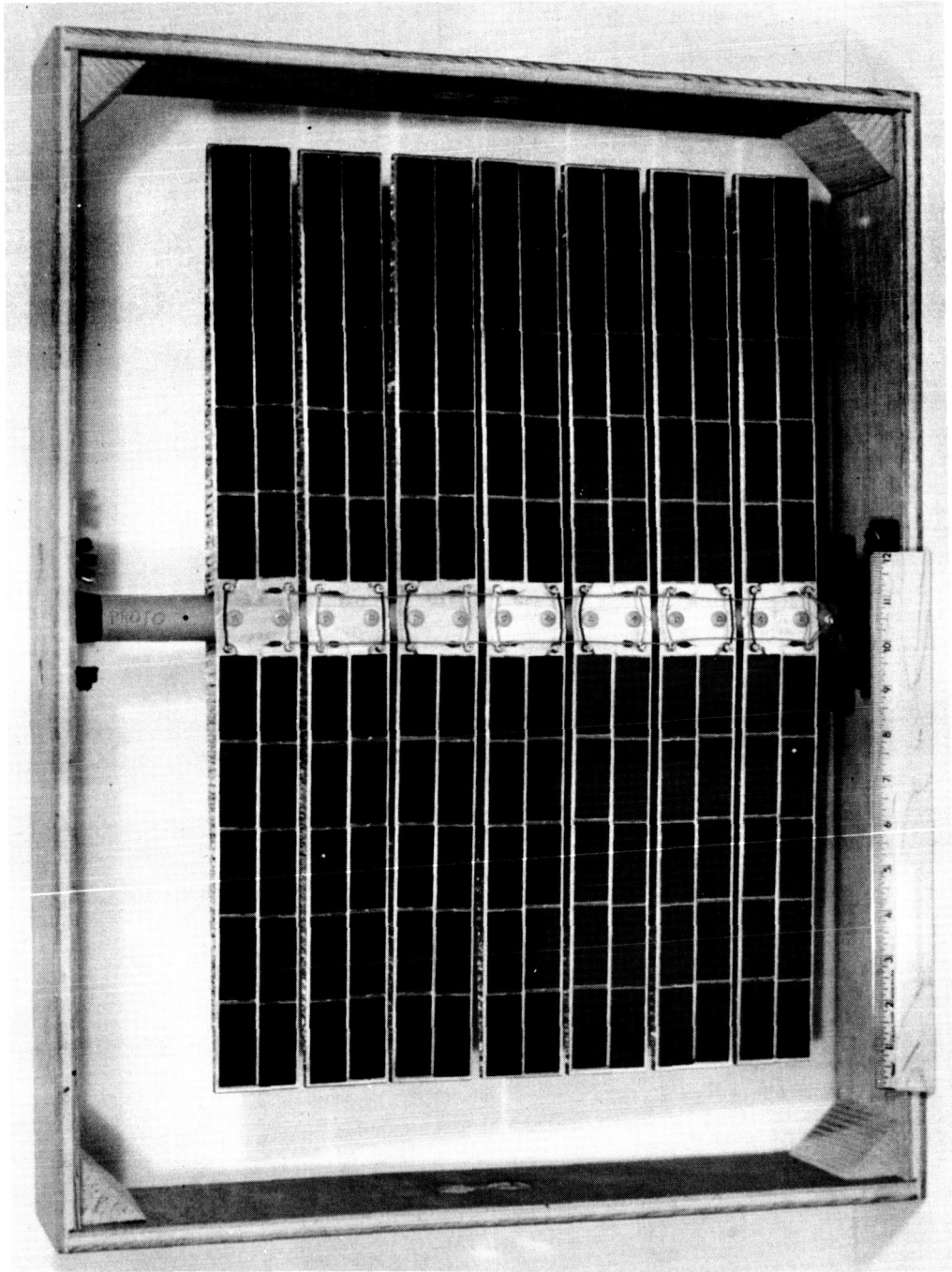


Figure 8—An Explorer XII Solar Paddle (in handling frame)

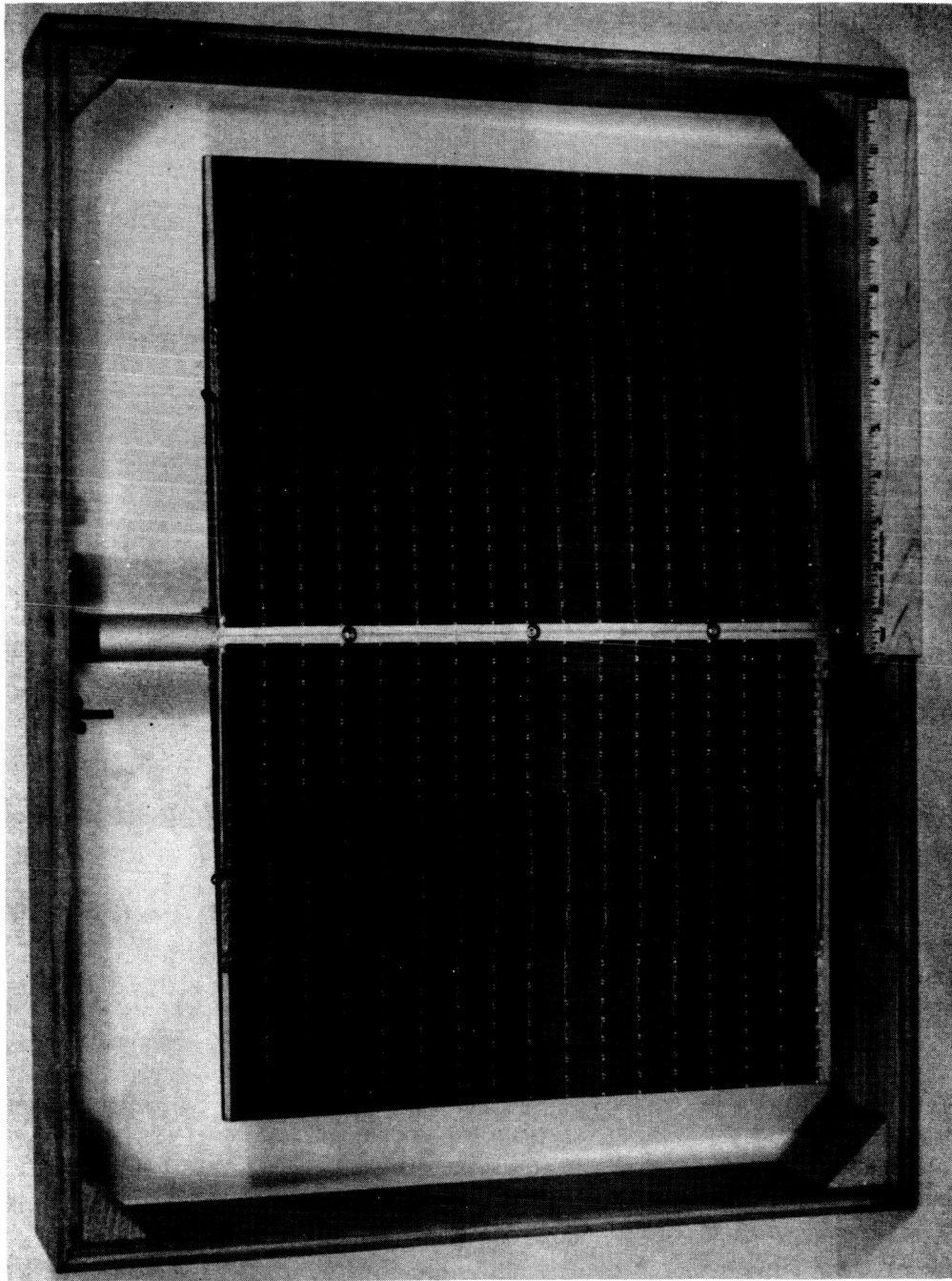


Figure 9—An Explorer XIV Solar Paddle (in handling frame)

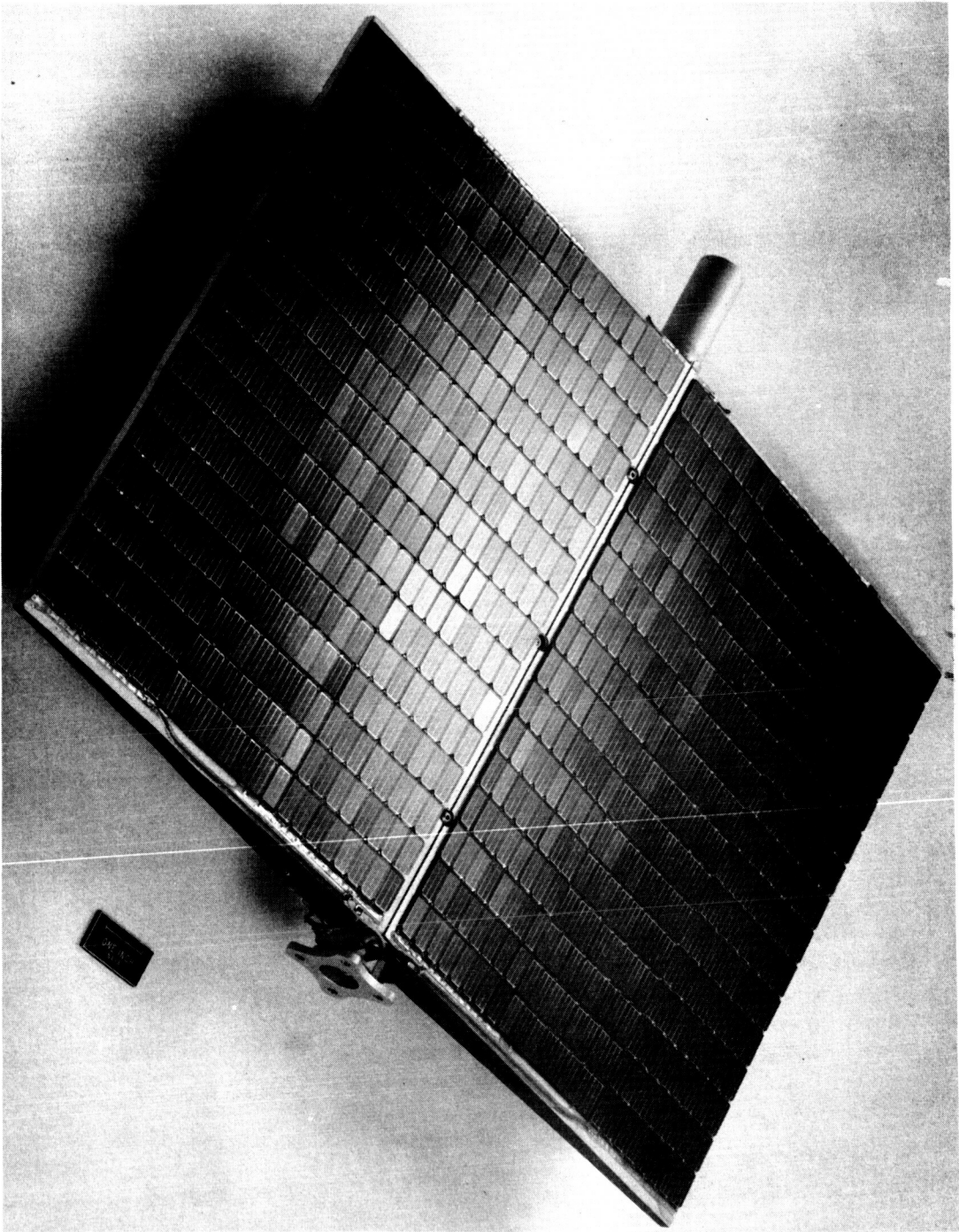


Figure 10—An Explorer XV or Explorer XXVI Solar Paddle

Significant changes were incorporated in the Explorer XIV paddle design (Figure 9). These changes were made to further increase the solar array output and to take advantage of significant developments in the state-of-the-art of both solar cell and solar paddle fabrication. The paddle substrate was changed to a two-module unit permitting a 48 by 8, series-parallel, flat-mount arrangement of the cells without changing the overall substrate envelope. By eliminating the wasted space between the previous modules, by the use of higher efficiency shallow-diffused, gridded solar cells, and with improved assembly techniques, it was possible to add the two extra series strings of cells to each paddle face. These changes resulted in an overall gain of approximately 45% in power, at a cost of only 16% in weight. In addition, the number of diodes per cell group was increased from 1 to 4, providing parallel redundancy. This only changed the total number of diodes from 14 to 16. The diodes were also moved from the surface of the paddle into the spar which provided additional radiation protection.

Because of the Starfish event, the change in orbit, and the crash basis - 53 days from inception to launch - upon which Explorer XV was designed and built, the only changes in these solar paddles (Figure 10) were the mandatory ones of high cell efficiency to compensate for the higher operating temperature (60°C as opposed to 0°C) and the use of heavier, 60 mil thick, glass cover slides for significantly increased radiation protection necessary in the new orbit and under artificial belt irradiations (see Table II).

There was no additional change in the solar paddles for Explorer XXVI since it was determined that the spare paddles from the Explorer XV spacecraft were to be used. (This spacecraft was basically the Explorer XV spare.) This determination was based on the estimate that the change to the "high-low" array with a long life requirement was compensated for by the decay of the artificial belt created by Starfish.

Table III
Solar Paddle Weights

Spacecraft	Paddle Weights (gms)				
	A	B	C	D	Avg.
Explorer XII	1256	1250	1256	1256	1254
Explorer XIV	1462	1427	1437	1493	1455
Explorer XV*	2367	2364	2361	2366	2364
Explorer XXVI	2355	2327	2338	2323	2336

*Including special balance weights within the substrate.

Table IV
Mechanical Characteristics of the Solar Paddles

Spacecraft	Paddle Substrate				Solar Cells			Cover Glass		Average Weight (gms)
	Length (in.)	Width (in.)	Area (ft ² per face)	Modules (no. per paddle)	Size (cm × cm)	Mounting (interconnection)	Number (per paddle)	Type (Corning)	Thickness (mils)	
Explorer XII	13.625	20.125	1.904	14	1 × 2	Shingle (series)	1400	0211	6	1254
Explorer XIV	13.625	20.125	1.904	2	2 × 1	Flat (series-parallel)	1536	0211	6	1455
Explorer XV	13.625	20.125	1.904	2	2 × 1	Flat (series-parallel)	1536	7940	60	2364
Explorer XXVI	13.625	20.125	1.904	2	2 × 1	Flat (series-parallel)	1536	7940	60	2336
NOTES	Aluminum honeycomb construction			Electroless nickel-plated contacts			Included blue-reflecting filter and antireflective coating		Average of four flight paddles	

Table V
Electrical Configuration of the Solar Paddles

Spacecraft	Solar Cell Configuration				Electrical Interconnection			Normal Incidence Space Power
	Type	Bare Cell Efficiency under Tungsten (%)	Diffusion	Gridding	Cells in Series (no. per group)	Cells in Parallel (no. per group)	Isolation Diodes (no. per group)	
Explorer XII	P/N	11	Deep	Ungridded	50	1	1	11.7
Explorer XIV	P/N	12	Shallow	Gridded	48	8	4	17.3
Explorer XV	P/N	13	Shallow	Gridded	48	8	4	19.0
Explorer XXVI	P/N	13	Shallow	Gridded	48	8	4	20.2

PADDLE POWER OUTPUT

The solar paddle power output was determined for loads varying between short circuit and open circuit to provide a complete current-voltage (I-V) curve for each paddle face. Measurements were made in sunlight on cloudless, haze-free (to the eye) days. For each successive spacecraft, the data were obtained using successively improved methods of measurement and correlation of the solar inputs and the paddle outputs as described in Appendix B. The resulting data for each paddle face and averages for each spacecraft are given in Table VI. In this table, it can be seen that there was an increase in power of approximately 45% from the Explorer XII to the Explorer XIV spacecraft. The approximate breakdown of this improvement is as follows:

a. Use of higher tungsten efficiency cells	10%
b. Use of shallow diffused ("blue") cells	10%
c. Use of additional cell strings	15%
d. Improved fabrication	<u>10%</u>
	TOTAL 45%

An additional 10% improvement in power output was realized for Explorer XV. This was almost entirely the result of the use of still higher efficiency cells. Further gains in power were realized in Explorer XXVI. Since these paddles were electrically identical to those of Explorer XV, it is evident that this gain was obtained because of operation at a lower temperature.

SOLAR ARRAY POWER OUTPUT

The space power output, prior to degradation, was predicted using both the quasi-theoretical and the empirical methods described in Appendix C. Theoretical aspect calculations were made for the Explorer XII satellite (Reference 1). These calculations apply equally, in terms of normalized effective paddle area, to Explorers XIV and XXVI because the array configurations are identical. The normalized effective paddle area of Explorer XV is, because of the "flat" configuration, simply $|4 \cos \psi|$ where ψ is the sunline - spin axis angle (defined in Figure 6). The normalized effective paddle area curves for these two configurations are shown in Figure 11. The normalized curve for the "high-low" array is converted into three power curves for Explorer XII, XIV and XXVI, and the normalized curve for the "flat" array, Explorer XV, is converted into a power curve in Figures 12 and 13, respectively. These curves are based on the average paddle power in Table VI. In addition, the Explorer XIV sun-spin test results and the

Table VI
 Calculated, Normal-Incidence, Space Power Output for the Solar Paddles

Spacecraft	Paddle Power (Watts)										Average	Design Temperature (°C)
	Paddle A		Paddle B		Paddle C		Paddle D		Face 1	Face 2		
	Face 1	Face 2	Face 1	Face 2	Face 1	Face 2	Face 1	Face 2				
Explorer XII	12.0	12.7	12.2	12.1	11.3	11.0	11.4	10.7	11.7	0		
Explorer XIV	17.5	17.3	16.9	16.8	17.7	17.5	17.3	17.5	17.3	0		
Explorer XV	18.5	18.7	19.2	19.4	18.9	19.1	19.3	19.3	19.0	60		
Explorer XXVI	20.1	20.2	20.6	20.2	19.7	20.1	20.5	20.2	20.2	30		

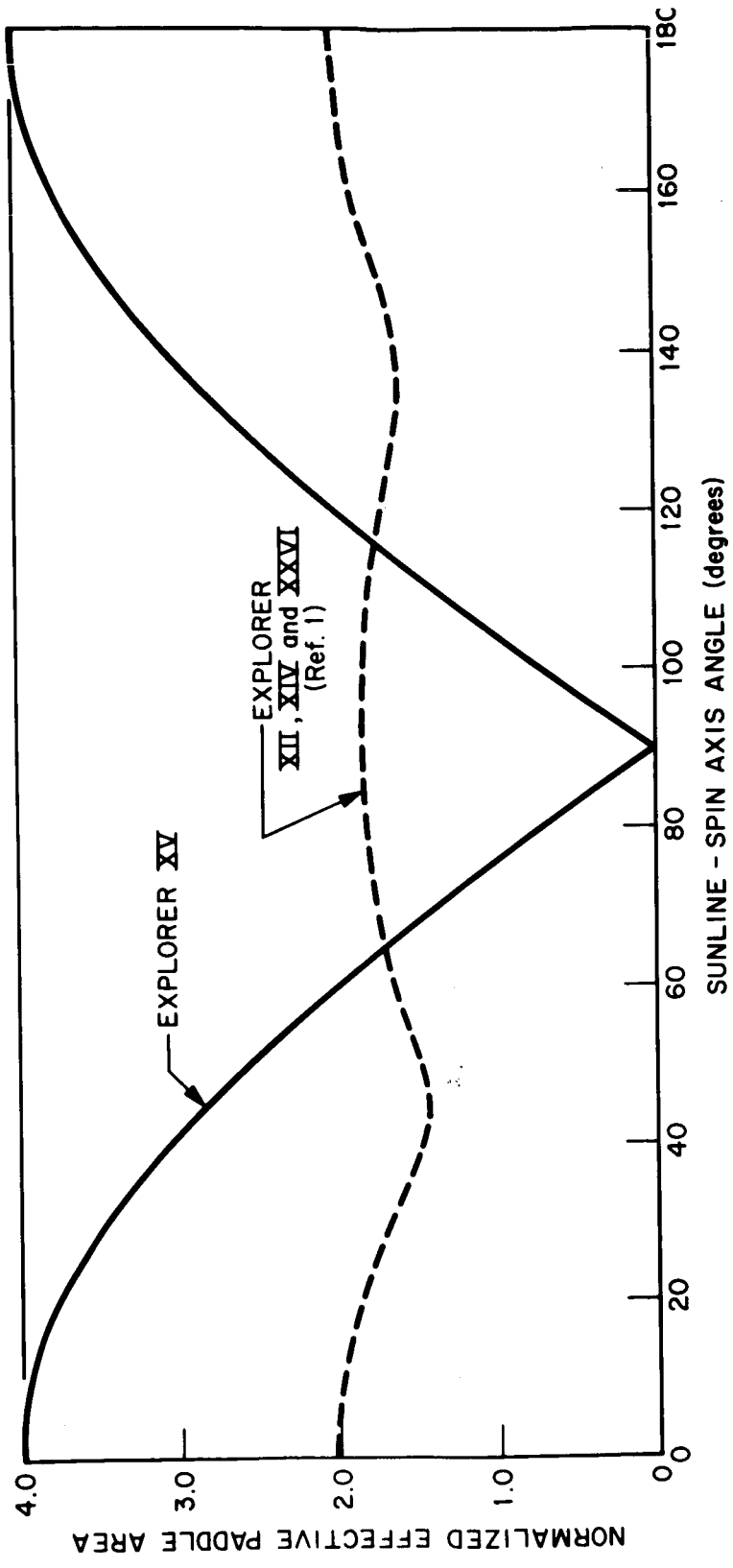


Figure 11 - Theoretical Effective Paddle Area

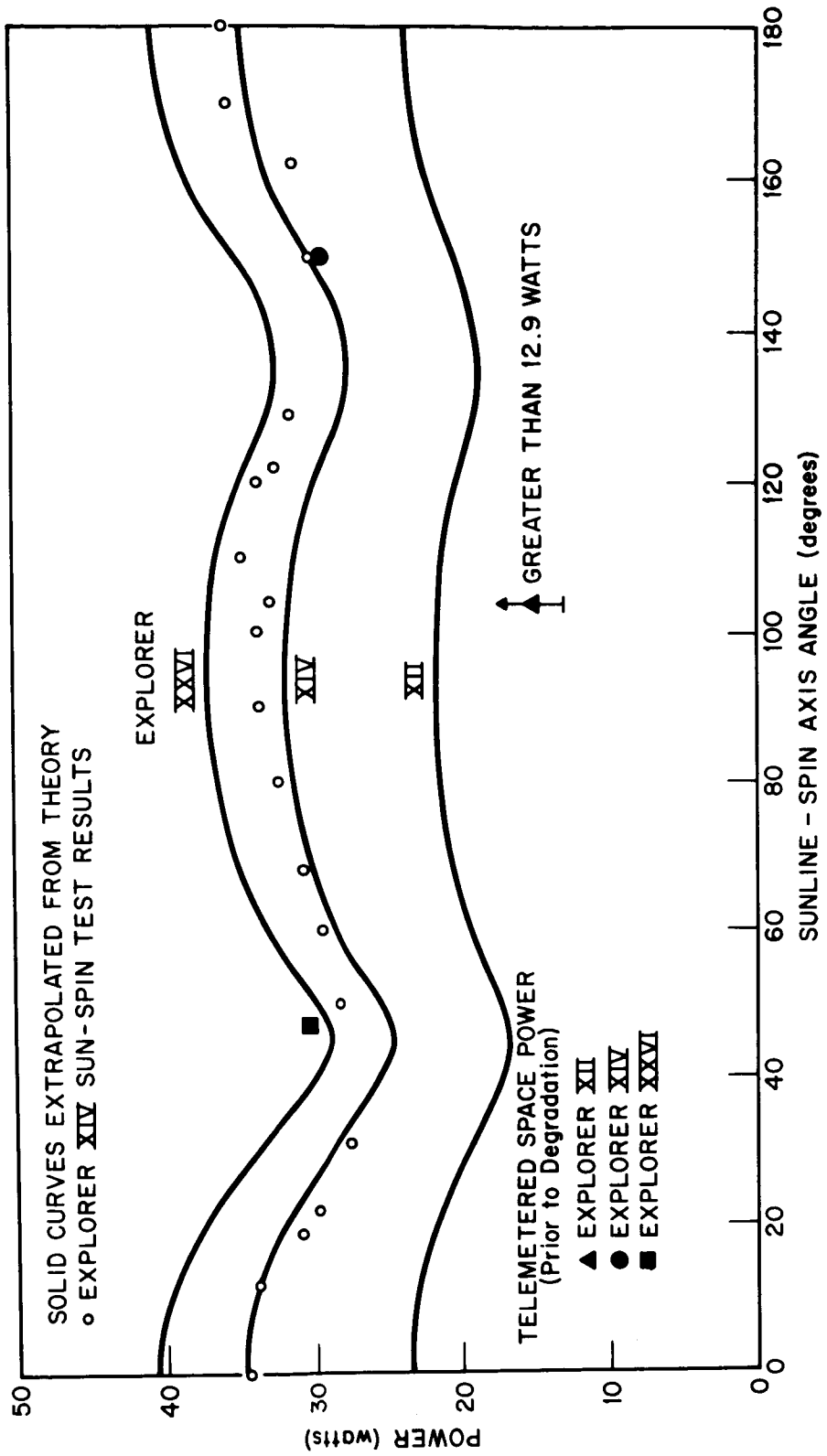


Figure 12—Space Power Output for Explorers XII, XIV, and XXVI

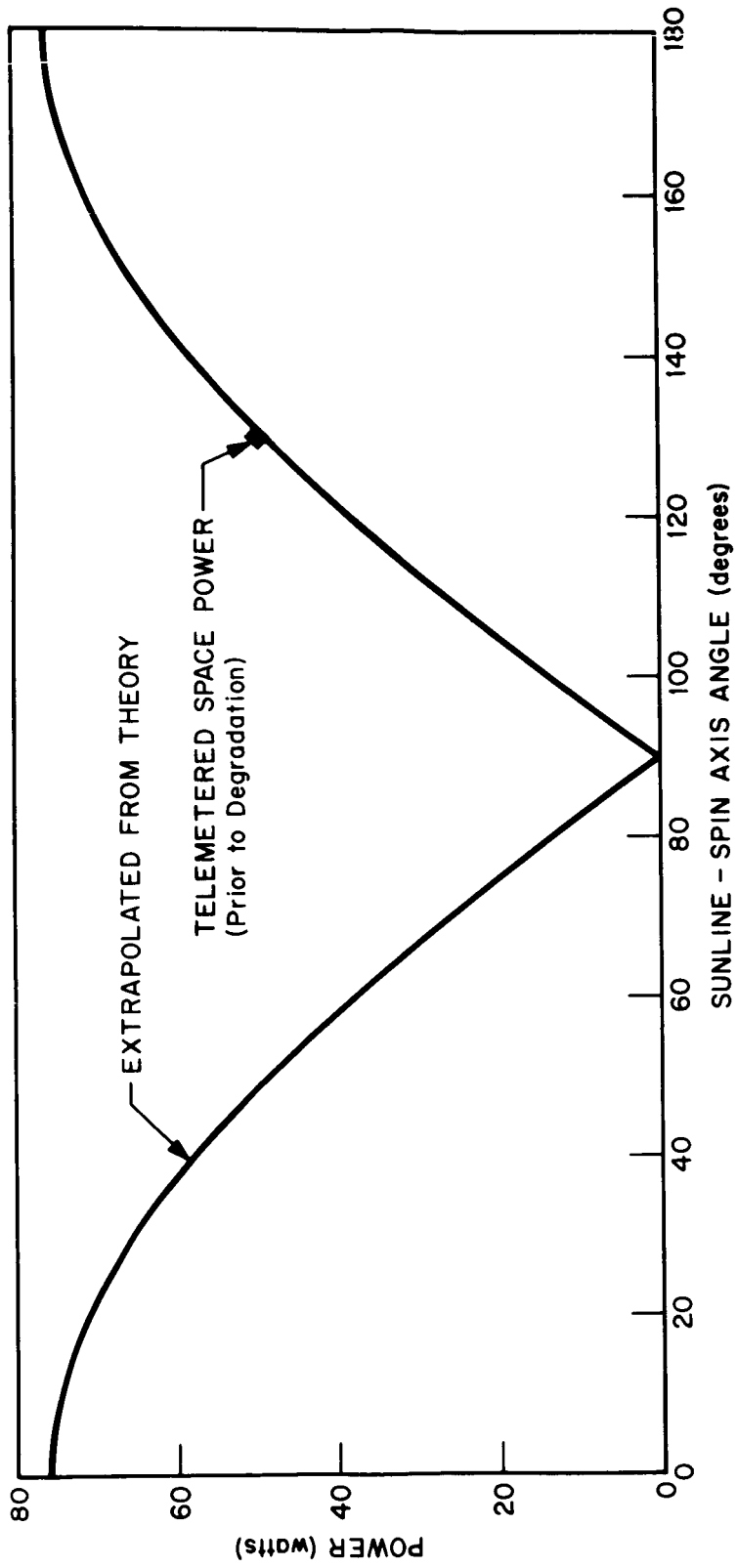


Figure 13--Space Power Output for Explorer XV

results of telemetered orbital data, prior to degradation of the solar arrays, are plotted in these figures for comparison. The orbital data are compared to the predicted data in Table VII. It can be seen in this table (and also in Figures 12 and 13) that the predicted power values were very close to the telemetered values. In fact, the values are much closer than can rightfully be anticipated since errors in prediction are estimated at approximately 10%.

Table VII
Comparison of Predicted Power and Initial Space Power

Spacecraft	Telemetered Data			Power Data		
	ψ (degrees)	V (volts)	I (amps)	Actual (watts)	Pre- dicted (watts)	Difference (percent)
Explorer XII	104	19.6	>0.66*	>12.9	21.4	---
Explorer XIV	150**	19.9	1.48	29.5	30.2	+2.4
Explorer XV	130	19.6	2.53	49.6	48.9	-1.4
Explorer XXVI	47	19.4	1.57	30.5	29.1	-4.6

*Telemetered current was paddle current minus shunt regulator current.

**Nominal in spacecraft precession with 9° cone angle.

GENERAL CHARACTERISTICS

General characteristics, of the type useful for feasibility studies and state of the art evaluations, are presented for the individual solar paddles and for the various spacecraft in Tables VIII and IX, respectively. Several items in these tables are worth special attention.

In Table VIII, it can be seen that the change from individual shingled cell strings on separate modules to series-parallel, flat-mounted cells on integral modules permitted a 14% increase in packing factor in spite of the fact that some area was lost because the cell contacts do not overlap. It is readily seen that this change of construction also increased the paddle weight. However, gains in

Table VIII
General Undegraded Solar Paddle Characteristics at Air Mass Zero

Characteristics	Spacecraft (Explorer Number)			
	XII	XIV	XV	XXVI
(1) Substrate Area (ft ²)	1.90	1.90	1.90	1.90
(2) Cell Area (ft ²)	1.39	1.65	1.65	1.65
Packing Factor (%)	73	87	87	87
(3) Weight (lbs)	2.77	3.21	5.21	5.15
(4) Density (lb/ft ²)	1.46	1.69	2.74	2.71
(5) Power (watts)	11.7	17.3	19.0	20.2
(1) Power Density (watts/ft ²)	6.16	9.10	10.0	10.6
(6) Specific Power (watts/lb)	4.22	5.39	3.65	3.92
(7) Cell Power (mw/cell)	16.7	22.5	24.7	26.3
(8) Cell Efficiency (%)	(9)6.63	(10)8.43	(10)9.29	(10)9.86

- NOTES:
- (1) Only one face of the paddle is considered. Entire rectangular envelope (excluding the extensions of the spar) is considered.
 - (2) Based on 9.2 cm² per shingle (four cells at 1.8 cm² and one cell at 2 cm²) and 2 cm² per flat-mounted cell.
 - (3) Entire paddle, including spar and flange for attachment to the spacecraft, is considered.
 - (4) Based on entire paddle weight and single face area.
 - (5) Under conditions of Table VI.
 - (6) Based on entire paddle weight and single face power.
 - (7) Only cells on and power from face toward and normal to the sun are considered.
 - (8) Computed from cell power and solar input of 140 mw/cm².
 - (9) Based on 1.8 cm² active cell area.
 - (10) Based on 1.9 cm² active cell area.

Table IX
General Solar Array Characteristics – Design Performance

Characteristics	Spacecraft (Explorer Number)			
	XII	XIV	XV	XXVI
(1) Array Area (ft ²)	15.2	15.2	15.2	15.2
(2) Array Weight (lbs)	11.1	12.8	20.8	20.6
Array Density (lbs/ft ²)	0.730	0.842	1.37	1.36
(3) Spacecraft Power (watts)	12.9	11.7	11.2	13.4
(4) Power Density (watts/ft ²)	0.849	0.770	0.737	0.882
(5) Specific Power (watts/lb)	1.16	0.914	0.538	0.650
(6) Normal Incidence Power (watts)	93.4	138	152	162
(7) Spacecraft Utilization Efficiency (%)	13.8	8.48	7.37	8.27
(8) Cell Power Utilization (mw/cell)	2.30	1.90	1.82	2.18
(9) Cell Utilization Efficiency (%)	(10)0.91	(11)0.71	(11)0.68	(11)0.82

- NOTES:
- (1) All eight paddle faces considered.
 - (2) Combined weight of four complete paddles including spar and connecting flange.
 - (3) Based on Table I.
 - (4) Based on design power and total array area.
 - (5) Based on design power and total array weight.
 - (6) Power capability for all 8 paddle faces normal to the sun.
Based on Table VI.
 - (7) Percent of normal-incidence power necessary to meet spacecraft power requirement.
 - (8) Power per cell necessary to provide spacecraft power requirement.
 - (9) Computed from cell power utilization and solar input of 140 mw/cm².
 - (10) Based on 1.8 cm² active cell area.
 - (11) Based on 1.9 cm² active cell area.

both power density and specific power, along with considerably increased reliability, more than compensate for the weight loss. The additional increase in weight after Explorer XIV is the result of the change from 6 to 60 mil glass slips. This weight penalty is, however, worthy of special note. It amounts to approximately 40% of the paddle weight.

The improvements in cell power and efficiency are representative of the state of the art of solar cells and solar paddle fabrication at the time of paddle design. Tremendous strides in both areas were achieved between 1960 and 1963. The air mass zero efficiency for a solar cell assembled on a paddle closely approached 10%.

In Table IX the most striking feature is the extremely poor utilization efficiency for cells mounted on fixed paddles on a spin-stabilized satellite with a shunt-regulated power system. These efficiencies, of less than 1%, are the result of four primary factors. The first is the capability for conversion of energy by the solar cell itself which is, after assembly, about 10%. The second is the orientation of the solar cells toward the sun in order to convert the energy. The third is the final utilization of this energy by the spacecraft. The fourth is the "fat" necessary in the design of the array to compensate for radiation degradation. Another important, but secondary factor is the safety margin required to allow for uncertainties in design and measurement. The end result of this combination is that the solar cells can convert approximately 10% of the solar energy into electrical energy, but because of misorientation, radiation degradation, etc., only about 14% of this conversion is accomplished and used by the spacecraft for paddles required to provide spacecraft power at end of life on an average basis and only about 8% for paddles required to provide this power under worst aspect conditions.

SUMMARY AND CONCLUSIONS

The preceding review and compilation of characteristics of the Explorer XII, XIV, XV, and XXVI solar arrays affords the following summary and conclusions:

1. Solar paddle and solar array characteristics, including both mechanical and electrical features, have been provided for four similar spacecraft and can readily be used in feasibility studies, etc.
2. Special features of the design of each array resulting from special requirements such as radiation environment, lifetime, state of the art, etc., have been described to show the dependence of solar array design on significant factors beyond the spacecraft power requirements.

3. The information presented provides a "picture" of state-of-the-art developments during the time period from 1960 to 1963. The developments include the following:

- a. Transition from multimodular toward unit substrate construction. (Single unit construction was not achieved.) This results in simplified construction.
- b. Change from series cell circuitry to series-parallel circuitry, resulting in increased reliability.
- c. Change from shingled solar cells to flat-mounted solar cells, resulting in increased reliability.
- d. Change from deep-diffused to shallow-diffused solar cells, resulting in increased efficiency in the "blue-shifted" AMO solar spectrum.
- e. Change from ungridded to gridded cells, resulting in increased efficiency.
- f. Increase of cell efficiency after assembly, from 6.6% to 9.9% at air mass zero.
- g. Addition of radiation protection for isolation diodes, resulting in greater stability.
- h. Addition of redundancy in the isolation diodes, resulting in increased reliability.
- i. Improvement of packing factor from 73% to 87%, resulting in increased power density and specific power.
- j. Increase in paddle power density from approximately 6 watts/ft² to approximately 10 watts/ft².

4. Initial space power data, telemetered from the spacecraft, show the design, measurement and prediction of solar array power to have been well within the 10% accuracy anticipated. Actual predictions were within 5%.

5. The paddle characteristics show that a tremendous weight penalty is paid for radiation protection. The penalty amounts to approximately 40% of the paddle weight when operation is to be in a high-radiation orbit.

6. Although solar cell efficiencies approached 10%, a summary of the general array characteristics shows the solar cell utilization efficiency (the power used as a percentage of the solar power which could be intercepted) is less than 1%.

RECOMMENDATIONS

The review of the information presented here leads to the following recommendations:

1. Since the utilization efficiency of the solar cells has been a miserable 1%, future efforts should be concentrated and increased in the following areas:
 - a. Orientation of solar arrays normal to the sun to eliminate presently lost power resulting from the solar cell intercepting only a small fraction of the solar input which it is capable of intercepting. Improvements can be made even in the case of spin-stabilized satellites.
 - b. Increased radiation resistance of solar cells to eliminate the initial "fat" required to compensate for radiation degradation. Higher radiation resistance will also reduce the exorbitant weight penalty previously encountered. Development and utilization of N/P solar cells and high base resistivity solar cells have, since 1963, produced significant gains in this area. Continued work on these and other cells such as drift field cells, etc., can increase these gains.
 - c. Elimination of shunt-regulation and inclusion of spacecraft power programming to provide for full utilization of available power. This can be partially accomplished by use of series regulation which maintains the solar array at its peak power point, but should be assisted by the combination of short-term and long-term experiments on the spacecraft with the short-term experiments being shut off successively as the array power degrades.
 - d. Reduction of solar array temperatures to provide for higher solar cell efficiency. This effort will become increasingly important as the degree of array orientation increases.
 - e. Improved methods and facilities for the prediction of space power in order to reduce the power contingency required to compensate for measurement uncertainties.

2. Since the solar array characteristics presented here afford a wide variety of information and since they are characteristics determined from actual flight hardware, it is recommended that they be used as a reference in future feasibility studies.

3. Since agreement, to the degree anticipated, has been found between flight data and data obtained by the extrapolation of air mass one measurements, made on individual paddles, to air mass zero utilizing theoretical aspect calculations, future efforts should concentrate on improving the theoretical calculations and improving the air mass one paddle measurements. Sun-spin tests will still be required to check the end results and to afford an all-systems test; however, because of inherent practical difficulties, they should not be used for "calibration" of the solar array.

ACKNOWLEDGMENTS

The authors wish to express their gratitude for the assistance, throughout the Energetic Particle Explorer projects, given by the many groups at GSFC that have aided in obtaining the information presented here. Special gratitude is expressed for outstanding cooperation and assistance from the Mechanical Systems Branch of the Goddard Space Flight Center.

REFERENCES

1. J. V. Fedor, Theoretical Average Available Power from S-3 Solar Paddles, Internal Memorandum, Mechanical Systems Branch, GSFC, July 25, 1961.

APPENDIX A
SPACECRAFT NOMENCLATURE

Each of the Energetic Particle Explorer spacecraft has been known by an Explorer designation and others. For clarification, the various names and designations given to these spacecraft are given below.

Table A1
Names and Designations of the Energetic Particle Explorers

Explorer Designation	Pre-Launch Designation	Alternate Designation
Explorer XII	S-3	-
Explorer XIV	S-3a	-
Explorer XV	S-3b	SERB
Explorer XXVI	S-3c	EPE-D

APPENDIX B
METHODS OF CORRECTING AND EXTRAPOLATING
EARTH SURFACE SUNLIGHT MEASUREMENTS
ON SOLAR PADDLES TO SPACE CONDITIONS

The method of determining space power output from earth surface solar paddle measurements is continually being revised and improved. Although the methods described below have been useful in their application, such was true only because the areas of inadequacy were recognized and compensatory allowances were made. It must be understood that these methods were those used in the past and under past conditions and are not considered satisfactory today.

The determination of space paddle power output consists basically of three steps. The first is to make paddle power and solar input measurements, the second is to correct these for extraneous effects, and the third is to extrapolate the data to space conditions. These procedures, as applied, are described below for the various spacecraft.

Explorer XII - The paddle was oriented with the surface in a horizontal plane. The solar input was obtained from the local U. S. Weather Bureau, where measurements were made using a 180° horizontal incidence pyrheliometer (pyranometer). The temperature of the paddle was determined by means of thermocouples taped at various points on the paddle.

It was assumed that both the solar paddle and the pyranometer respond in the same manner to the various inputs (direct sunlight, sky radiation, stray and reflected light). It was also assumed that the space solar input was effectively (allowing for spectral differences) 117 milliwatts per square centimeter. (This factor has become fairly standard as a nominal, conservative extrapolation factor.) The paddle power, corrected for temperature (to be described later), was then linearly extrapolated according to the equation:

$$P_0 = \frac{117 P}{H} \quad (B1)$$

where P_0 = space (or air mass zero) power output at normal incidence.

H = horizontal incidence pyranometer reading (in mw/cm^2)

P = measured paddle power output after correction for temperature.

Explorer XIV - The paddle was oriented normal to the sun in a black box enclosure (15' by 15' in area and 12' in height). The solar input was obtained using a normal incidence pyrhelimeter. The temperature was determined by means of a calibrated thermistor taped to the paddle.

It was assumed that the solar paddle output was enhanced 10% by extraneous light inputs. The paddle power, corrected for temperature, was therefore reduced 10% and extrapolated linearly according to the equation:

$$P_0 = \frac{117 (0.90 P)}{N} \quad (B2)$$

where N = normal incidence pyrhelimeter reading (in mw/cm²).

Explorer XV - The solar paddle was mounted normal to the sun. The input was measured using a 180° incidence pyranometer also mounted with the sensing surface normal to the sun. The paddle temperature was estimated.

The method used for extrapolating the measured data for this spacecraft was identical to that for Explorer XII.

Explorer XXVI - The solar paddle was mounted normal to the sun in the black box enclosure. Solar input and stray light input were determined using both a normal incidence pyrhelimeter and a 180° horizontal incidence pyranometer. In addition, the sun angle to the zenith was measured. The paddle temperature was determined using a calibrated thermistor taped to the solar paddle.

It was assumed that the solar paddle was affected proportionately, and with the same efficiency factor, by the two independent illuminations - the direct solar input and the stray light - and that the power output was the result of the two illuminations combined according to the equation:

$$P = \eta (N + S) \quad (B3)$$

where N, the normal incidence pyrhelimeter reading, is taken to be the direct solar radiation, S = stray light (in mw/cm²), η = conversion efficiency factor. Also, if it were possible to make completely collimated measurements, the space power output would be determined from the equation:

$$P_0 = \frac{117 P_c}{N} \quad (B4)$$

where P_c = paddle output under collimation. But,

$$\frac{P_c}{N} = \eta \quad (B5)$$

So,

$$P_0 = \frac{117 P}{N + S} \quad (B6)$$

The value of $(N + S)$ was found from the pyrliometer and pyranometer measurements, assuming that their responses were similar to that of the solar paddle. In addition, it was assumed that the input to a horizontal surface (the 180° pyranometer) was the combined input from direct solar radiation and from stray light and that the output or response was proportional. In this case, the solar input is at an angle to the sensing surface and only the component normal to the surface is considered and gives rise to the following equation:

$$H = N \cos \alpha + S \quad (B7)$$

where H , the pyranometer reading, is taken to be total radiation on the horizontal surface. α = sun angle to the zenith. This gives:

$$N + S = H + N (1 - \cos \alpha) \quad (B8)$$

Equation B6 then becomes:

$$P_0 = \frac{117 P}{H + N (1 - \cos \alpha)} \quad (B9)$$

This equation provides for the calculation of the space power output in terms of the measured parameters.

Whenever the solar paddle output was measured at a temperature significantly different from that predicted for orbital operation, it was necessary to correct the measured paddle output for the temperature effects. To make this correction, the current variation with temperature was disregarded as negligible and only the voltage variation with temperature was considered. The intended operating voltage was corrected according to the following equation:

$$V_1 = V_{op} + \alpha n \Delta T \quad (B10)$$

where V_1 = the corrected voltage,
 V_{op} = the intended operating voltage,
 α = the temperature coefficient of voltage (-2.4 mv/cell/°C),
 n = the number of cells in series,
 ΔT = the temperature difference ($T - T_0$),

where T = the temperature of the paddle at the time of measurement, and
 T_0 = the predicted temperature for orbital operation.

The current on the I-V curve was read at the voltage V_1 and the corrected power was calculated using the equation:

$$P = I V_{op} \quad (B11)$$

where P = the corrected power output, (at AM1), and
 I = the current at V_1 from the I-V curve.

APPENDIX C

SOLAR ARRAY CALIBRATION

For any irregular configuration of either the solar array or the spacecraft, the output is dependent on the orientation of the satellite with respect to the sun. This includes both satellite axis-sunline orientation and also the rotation of the satellite about its axis. Several methods of calibrating the solar array output against orientation and rotation have been used.

Quasi-Theoretical Method - In this method the effective paddle area (the projected area in a plane perpendicular to the sunline) is calculated theoretically. The approximate effect of shadows (due to overlapping of paddle on paddle or spacecraft on paddle) is subtracted out and the resulting curves of area versus orientation are plotted in terms of normalized effective paddle areas. The output of the solar paddles is measured in sunlight, corrected for temperature, extrapolated to a normal incidence space (air mass zero) value, and averaged. The area-orientation curves are then scaled to power-orientation curves using the air mass zero power figure.

Photographic Method - This method is identical to the Quasi-Theoretical Method except that the paddle areas and shadow effects are determined by means of photography, using as large a distance between camera and spacecraft as possible to eliminate parallax.

Empirical Method - In this method the spacecraft is assembled on a spin table and rotated in sunlight. Readings of the solar array output as a function of rotation are obtained for various sunline to spin-axis angles and the results are corrected using a nominal measurement of the output due to backlighting of a paddle and are then extrapolated to air mass zero conditions.

Table C1 provides a comparison of the primary advantages and disadvantages of each of these methods of calibration.

Table C1
Comparison of Methods for Space Power Output Calibration

Method	Advantages	Disadvantages
Quasi-Theoretical	<p>Desk calculations possible.</p> <p>Applicable to all configurations.</p>	<p>Shadow effects are estimated.</p> <p>Deviation from cosine law is not taken into account.</p>
Photographic	<p>Shadow effects are obtained in detail.</p> <p>Camera with telephoto lens provides collimation.</p>	<p>Tedious measurements (with some loss in accuracy) of photographic results.</p> <p>Deviation from cosine law is not taken into account.</p> <p>New measurements required for each configuration change.</p>
Empirical	<p>Curves are obtained directly.</p>	<p>Large errors occur from reflection and backlighting. (Collimation is not possible.)</p> <p>Requires excellent weather.</p> <p>New measurements required for each configuration change.</p> <p>Temperature corrections are not readily made.</p>